

Seismic Data Acquisition and Processing



Kabir Roy Chowdhury
Department of Earth Sciences, Utrecht University, Utrecht,
The Netherlands

Definition

Seismic data acquisition	Generation of (artificial) seismic signals on land (on surface, or, buried) or in water, reception of the signals after their travel through the interior of the earth, and their (digital) recording for later analysis.
Seismic data processing	Analysis of recorded seismic signals to filter (reduce/eliminate) unwanted components (noise) and create an image of the subsurface to enable geological interpretation and eventually to obtain an estimate of the distribution of material properties in the subsurface (inversion).

Introduction

Reflection seismics is akin to the “echo-in-the-well” experiment, it involves calculating the depth of the geological boundary from the two-way traveltime (TWT) of the seismic signal and its speed.

Seismic data acquisition and processing aims mainly to obtain an image of the sedimentary basins in interior of the earth, using waves generated by “artificial” earthquakes. These images can then be used to identify locations favorable for accumulation of hydrocarbons (oil and gas), which may then be drilled to determine the ground truth – and eventually to exploit the resources. Since the first known reflection seismic experiment in 1921 near Oklahoma City, USA (Fig. 1.3, Sheriff and Geldart (1995)), reflection seismics

has established itself as the most accurate technique to image the sedimentary basins for the exploration of hydrocarbons.

The phrase “seismic” instead of “seismological” in the following stresses the “man-made” nature of the waves used. Both seismics and seismology use the basic theory of wave-propagation through the earth, for which Aki and Richards (2002) is a good resource. Table 1 summarizes the important differences between the two approaches though; let us briefly look at two.

Frequency vs. period: Due to the spectral range of the signals involved, seismology traditionally uses period (s) to describe the waves, whereas in seismics, frequency (Hz.) is used. Waves provide information about the medium through which they propagate at the scale of their wave-length, and use of higher frequencies in seismics (shorter wavelengths) leads therefore to a greater resolution (of the structure) compared to seismology.

Wave-propagation: Seismology – again historically – mostly uses refracted energy, whereas exploration seismics is often synonymous with reflection seismics, although refraction seismic exploration predates the latter.

It may be noted, however, that recently there has been a blurring of the boundaries between the two fields. This has been driven by progress both in the instrumentation (acquisition) and in theory (processing). Seismologists are increasingly using higher frequencies and reflected wavefields, and practitioners of reflection seismics are using lower frequencies and refracted phases – both with the aim to improve the imaging of their respective targets. Italicized items in Table 1 are thus changing with time.

A similar comment applies also to “noise.” Considered earlier to be a bane of imaging, it is being increasingly used in innovative ways to optimize acquisition and improve imaging; this aspect will be briefly dealt with later.

This essay will be mainly concerned with acquisition and processing of reflection seismic data. Note, however, that seismics is being increasingly applied to both shallower

Seismic Data Acquisition and Processing, Table 1 Imaging the earth using natural/artificial earthquakes

Keyword	Seismics	Seismology
Wave source	Explosions, vibrations	Natural earthquakes
Energy penetration	Shallow	Deep
Max imaging depth	Base of crust	Whole earth
Location of source	Precisely known	Estimated postfacto
Time of occurrence	Precisely known	Estimated postfacto
Energy involved	Small-medium	Can be huge
<i>Wave propagation</i>	Mostly vertical	Mostly horizontal
<i>Frequencies mostly excited/used</i>	1–100 Hz	0.01–1 Hz.
Receivers	Geophones	Seismometers
Wave-field sampling	Dense	Sparse (getting better)
Data volume	Terrabytes	Gigabytes
Accuracy	Large	Small-medium
Main application	Oil and gas	Earth-structure
Other applications	Civil engg., crustal	Civil engg.
Investment	\$\$\$\$	\$\$

\$\$\$\$ Very → expensive; \$\$ → Expensive

depths (high resolution seismics) and crustal-scale studies down to Moho and beyond (deep seismics), see ► [“Deep Seismic Reflection and Refraction Profiling”](#) for details of the latter. Seismic Data Acquisition and Processing is a broad subject, the treatment here will have to make choices based upon space constraints, etc. Some subtopics, for example, ► [“Seismic, Migration”](#) are, however, dealt with in separate essays in this volume. This essay has been updated for the 2nd edition by briefly indicating relevant advances and including references for the same. The adjective “classical” has been used at places to indicate possible recent changes of the subject/term under discussion.

The reader is assumed to be familiar with the basic theory of elasticity and wave-propagation and the related concepts of reflection, refraction, and scattering. The concept of rays will be frequently used – especially in illustrations – for convenience; real seismic signals are of course associated with wave-fronts. Similarly, the figures will depict a 2-D section of the 3-D earth.

There are many good resources available even for the narrower field of Reflection Seismic Data Acquisition and (Signal) Processing, for example, Vermeer (2002), Yilmaz (2001), Menke (1989), Liner (2004), and Sheriff and Geldart (1995); the last one also contains some historical background and material over refraction seismics. Recently, some resources have also been made available for downloading on the Internet, for example, Claerbout (1985a, b).

Seismic Data Acquisition and Processing, Table 2 sources and receivers used in seismic surveys

Environment	Sources	Receivers
Land	Explosives/vibrators/impact/noise	Geophones
Marine	Air/water-guns	Hydrophones/nodes
Water-bottom	Explosives/guns	Nodes/geo/hydrophones
Onshore-offshore	Explosives/guns	Geo/hydro-phones

In this entry, all-capitals will be used to denote acronyms for jargons, of which there are quite a few (e.g., TWT above), and italicized phrases within double quotes will refer to articles elsewhere in this volume, for example, ► [“Propagation of Elastic Waves: Fundamentals”](#).

Seismic Data Acquisition

Before seismic signals can be processed, an artificial wavefield has to be generated using suitable *sources* at appropriate locations, measured by suitable *receivers* at other locations after getting reflected back from within the earth, and stored using *recorders*. Several technical and financial parameters have to be considered to obtain optimal data, for example, dense spatio-temporal sampling, power-supply, timing accuracy (GPS?), and – increasingly – HSE (Health–Safety–Environment) aspects. Design of a seismic survey (*geometry*) needs inputs from regional geology, exploration objectives, and logistical considerations.

At first confined to land, seismic surveys are now-a-days carried out mostly in marine environments in round-the-clock operations using large vessels and a lot of instrumentation; single-channel seismics has faded away in favor of multi-channel acquisition, allowing much more information to be obtained (see ► [“Single and Multichannel Seismics”](#)). Table 2 gives an overview of the equipment used under different field environments.

Several interesting theoretical- and practical-advances have been made recently in the field of seismic data acquisition and processing. These include *simultaneous* recording of wavefields *overlapping* in time and use of *noise as signal*. These will be briefly described towards the end of this entry.

Seismic Sources

One needs a signal that is high in energy (amplitude) to ensure a good depth penetration and short in duration to ensure accurate determination and *separation* of the travel-times – a Dirac-Delta spike would be ideal, possessing perfect resolution, it is however a-causal. In practice, a sharp, compact, and *repeatable* signal is preferred. This quasi-idealized waveform, possessing finite temporal duration and frequency

band-width (both with respect to the ambient noise), is called a *wavelet*. The source wavelet changes form as it travels through the earth due to several physical processes to be briefly discussed below – much of the later data processing aims to undo these changes.

Repeatability of the source wavelet – that is, that of its *amplitude* and *phase* content is an important pre-requisite for the later processing steps. Explosives were the initial choice for source on land, providing large energy (good depth penetration) but having non repeatable signal shape and negative environmental impact. Development of large, truck-mounted electro-mechanical vibrators have led since 1960s to their increasing use in land-seismics, with both the above disadvantages of impulsive sources reduced significantly.

In marine environment, compressed air is used – with explosion (*air gun*) or implosion (*water gun*) – to create the acoustic waves. The sources are towed by a ship together with the receivers (*single vessel seismic*) or by a separate ship (*two-ship seismics*).

There have also been experiments with shear-wave sources – both impact-type and vibratory. These – either alone or together with compressive sources – can provide extra information about the subsurface medium. For investigating shallower structures in engineering, environmental, and archeological applications, small impact-based sources, for example, weight-drops, rifles, and even portable vibrators are being frequently used and provide the required higher resolution.

Seismic Receivers

All land-seismic (and seismological) receivers (*geophones*, *seismometers*) are electro-mechanical devices that transform the relative motion of the medium in which they are embedded, into electrical voltages. Fidelity of this transformation – both in *amplitude & phase* is important to ensure maximum information retention for later retrieval – a flat amplitude response, with no phase distortion within the band of frequencies that are of interest, would be ideal. The output of such devices can be made to be proportional to the displacement/velocity/acceleration associated with the causative motion. Dennison (1953) provides an overview of the physico-mathematical underpinnings of geophone design; see also ► “Seismic Instrumentation”.

Originally, geophones were designed to move – and hence record information – only in the vertical direction. Later, the importance of recording and analyzing the entire three-dimensional elastic wavefield came to be realized. Multi-component receivers, enabling recording/analysis of both horizontal components, or all three spatial components of the ground movement are being increasingly used even in large scale surveys.

For use in water, small piezo-electric elements – hydrophones – are employed to record pressure variations – modern

deployments typically consist of thousands of such elements being towed near the water surface by *streamers*, several kilometers long, which are liquid-filled plastic tubes, fitted with fins (for buoyancy), gps receivers (for location information), and fiber-optic cables (to transfer the data) to the ship.

Three-component receivers may be deployed together with hydrophones at the water bottom (4C), to record the wavefield across it, see ► “Ocean Bottom Seismics”. Advances in this area have resulted in cable-free autonomous “nodes” – for both marine- and land-environments, for example, Dean et al. (2018). Besides saving cables and manpower (read: *cost*) for their deployment, they allow for complex acquisition geometries, large recording distances, and are also environmentally friendly.

Note that both sources and receivers may be deployed in *groups*, using specific patterns, which affect the generation and sampling of the wavefield due to their direction-dependent radiation/reception characteristics.

Seismic Recorder

The time-varying electrical signals output by the receivers represent *arrivals* back-scattered from different depths, all juxtaposed in time, and embedded within the ever present background noise and require storage for later processing. In the beginning, photographic films and later magnetic tapes were used for this purpose. The digital revolution starting in the 1960s, itself partly driven by the needs of seismic data-acquisition and processing, caused a complete shift to in situ digitization and digital storage. Similarly, the wires connecting the receivers to the recorder have been mostly replaced by fiber-optic cables or wireless. Modern 3-D seismic surveys record four-dimensional data – two each for sources and receivers; repeat surveys (*time-lapse seismics*) even add a fifth dimension.

Preserving the frequency, amplitude, and phase of the signal and the desired *dynamic range* are important considerations in designing the digitizing (*sampling*) unit. Digitization of this vast amount of data (wavefield) has traditionally been done honoring the *Nyquist Sampling Criterion*, which requires a uniform sampling rate of more than twice the highest frequency – or wavenumber – depending upon the domain (time/space) – present in the data. Sampling below the Nyquist rate produces artifacts (called aliases) in the digitized data at lower frequencies (or wavenumbers) and can eventually interfere with real signals that may be present there – see Claerbout (1985a) or Menke (1989) for details.

Theoretically, Nyquist rate sampling allows the reconstruction of the uniformly sampled wavefield using an infinite integral – which, clearly, is not practical. Hence, the signal received at each receiver location is usually over-sampled (e.g., at twice- or higher-Nyquist rate) to maintain high-fidelity while reconstructing the wavefield from the traces with a finite effort, without loss of information. Spatial

sampling of the seismic wavefield is seldom regular and uniform and produces “gaps,” which need to be filled by interpolation; this will be briefly discussed in a later section.

Recently, the necessity of acquiring seismic data at- or above-the Nyquist criterion has come under critical review – especially in view of the resultant massive increase in the data volume. An interesting development in this field has been included towards the end of this entry.

As each *receiver (group)* corresponds to a different *channel* in the recorder, digitization in such systems (typically consisting of thousands of channels) must preserve the time-base, to enable comparison of the arrival-times between different *traces*. Also, the actual instant of the *shot* – t_0 – must be transferred from the source to the recorder and recorded; it is often used to start the recording process itself, as seismics is only interested in travel-times, that is, arrivals-times with respect to t_0 . The digitized data – uniformly sampled time-series – from each individual experiment (*shot*), consisting of multiple *traces* (output of receivers) is called a *seismic record*.

Acquisition Geometry

Assuming a *layer-cake* model (sedimentary beds parallel to the surface), early surveys deployed a number of sources and receivers along a straight line on the earth-surface to obtain a vertical cross-section of the geology below this line (*2-D*).

Figure 1 shows schematically the approach in such a survey and is – in spite of its simplifications – useful in understanding several basic ideas. All the five panels show the earth-surface at the top, and a reflecting boundary (*target*), parallel to it, at some depth. Numerals on the surface represent surveyed equi-distant flag-positions to denote locations. The top panel shows the first measurement, with the source at “0” and eight receivers at locations “1” thru “8”. Assuming a homogeneous and isotropic medium, the paths predicted by Snell’s law for a part of the source energy to first travel downwards to the target and then reflect upwards from it to reach the receivers are indicated by the oblique lines.

The signals output from the receivers are digitized in the recorder to yield a *seismic record*, that is, a collection of *seismic traces*. Such an ordered collection of seismic traces is called a *gather*; having a common *source*, the record resulting from our first measurement is a *common source gather* (CSG_0), the suffix denoting source position.

Under the twin-idealizations of no background noise, and a spike-like source signal, each channel in the recorder (*seismic trace*) will consist of one single blip corresponding to the arrival time of the signal; in reality, the arrivals will have random background oscillations due to noise, and one *wavelet* corresponding to the single reflection arrival. Assuming constant speed of propagation v and depth to the target H , it is trivial to show (e.g., Sheriff and Geldart 1995) that the travel-times to the receivers can be written as $t_x^2 = (x^2 + 4H^2)/v^2 = t_0^2 + x^2/v^2$, t_x being the arrival-time

recorded by a receiver at a source-receiver *offset* of x . The travel-time curve for such a situation is thus a hyperbola – this simple relationship underlies much of seismic processing. t^2 plotted against x^2 thus yields a straight line, the slope being v^{-2} , that is, square of the *slowness* of the medium. Note that in seismics the *velocity*, which sensu-stricto is a vector, is almost always used to denote the local wave *speed* (a scalar), which is a property of the medium (rocks) . . . we shall follow this usage.

Our aim is to find H , the depth to the target ($= t_0/2v$). We have thus to estimate t_0 from the rest of the reflection hyperbola. Note that the reflection points on the target for the different receivers are different.

Hence, in what has become almost universal practice, the measurement is repeated after shifting the whole set-up laterally along the measurement line, keeping all the relative distances the same. In panel 2 of Fig. 1, the source and the receivers have been shifted right by one unit; only a few ray-paths are shown for this gather (CSG_1). Similarly, gathers CSG_2 and CSG_3 are also measured and recorded. During these measurements, the same receiver locations recorded signals from different sources, so that a postmeasurement re-arrangement of the traces could also yield *common receiver gathers* (CRG), in our case we would obtain CRG_1 – CRG_{11} ; these are useful for certain processing situations.

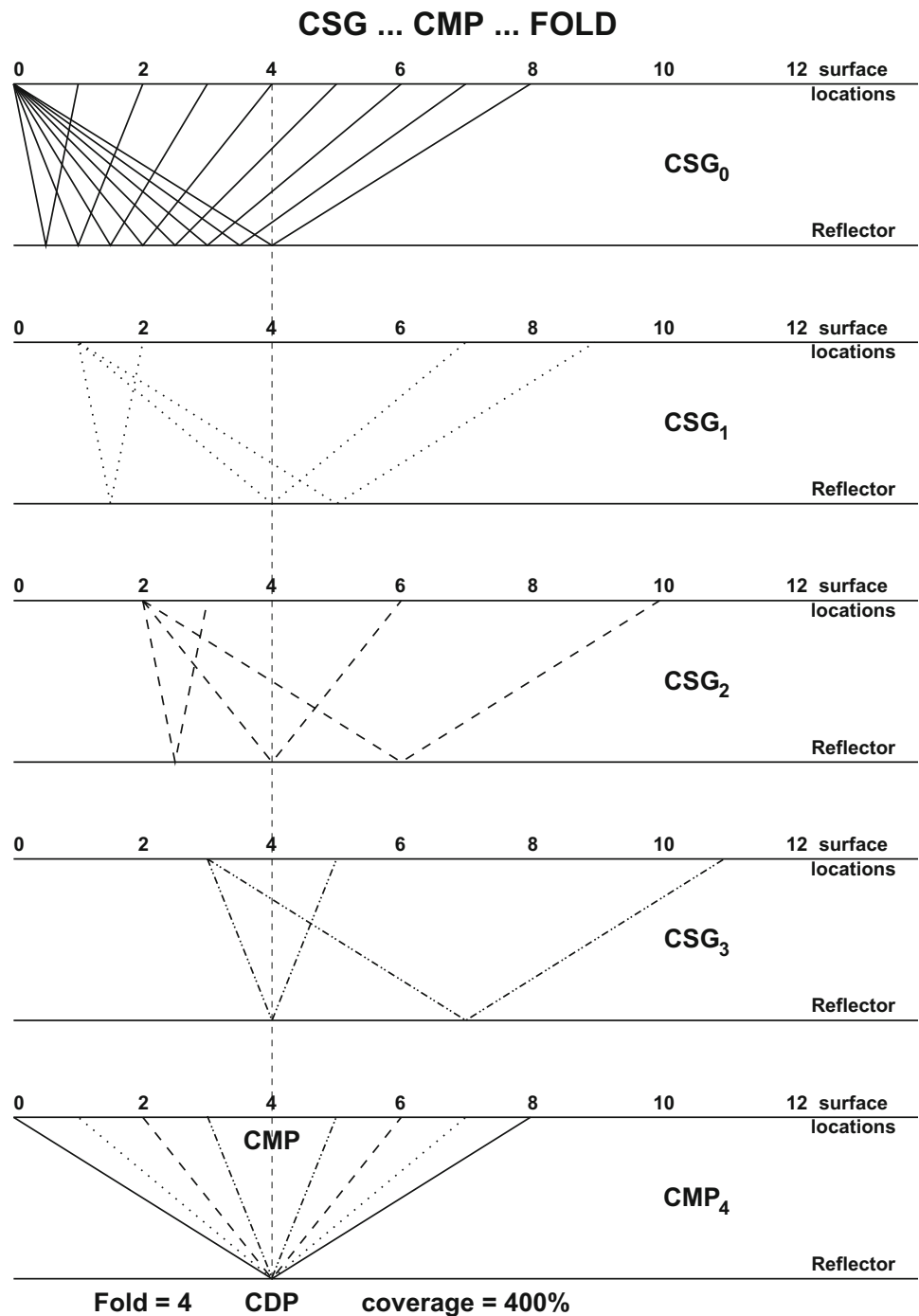
The lowest panel of this figure shows a special kind of resorting, collecting the traces from the four *shots* with one *common reflection point* (CRP). Four traces corresponding to source/receiver combinations of 0/8, 1/7, 2/6, and 3/5 were selected respectively from the four gathers. For our simple geometry, the four ray-paths shown share two things – a *common mid-point* (CMP_4) between their respective source and receiver locations and the *common depth point* (CDP) at the target depth, the latter being the same as CRP. Such a gather is called a *CMP-gather* and indexed by the position of the CMP. The travel-time plot of the reflection arrivals in a *CMP-gather* is also a hyperbola.

The four ray-paths shown for the gather CMP_4 all have the same reflection point and thus contain information about the same subsurface geology. The arrival times of the reflection signal in the four traces are of course different, as the travel paths are different. If this difference is corrected for, then adding the four traces should increase the coherent signal (information regarding the CRP) with respect to the *random* noise. The improvement of S/N by adding N traces is given by

$$\frac{\sum(\text{N traces with identical signal})}{\sum(\text{N traces with random signal})} \approx \frac{N}{\sqrt{N}} = \sqrt{N}.$$

The improvement of the signal-to-noise (S/N) ratio is thus roughly proportional to the square-root of the number of traces added. This number (4 in our case) depends upon the

Seismic Data Acquisition and Processing, Fig. 1 Schematics of seismic data acquisition by common-mid-point (CMP) profiling. Panels CSG_0 through CSG_3 represent common-source-gathers (CSG); CMP_4 is a common-mid-point gather for one common-depth-point (CDP). See text for details



survey geometry and is called the *fold* of the survey. Starting from fold 1 for $CMP_{0.5}$ (not shown), it gradually builds up to its nominal value (4 in this case) and again drops off at the other end of the survey.

Acquisition configuration can be specified by expressions describing the position of the source relative to the receivers viz. *end-on*, *split-spread*, *broad-side*, etc. Depending upon the geology and the noise regime, these configurations, as also varying *fold*, leave subtle but important *footprints* on the data.

In reality, the geology is of course not as in Fig. 1, and presence of structure (*dips*, *faults*, *folds*, etc.) is what makes hydrocarbon accumulation possible in the first place. Processing of 2-D data can remedy this situation – though only partially. Availability of more equipment and data-processing power led therefore to development of 3-D acquisition, with receivers laid out on the surface in a 2-D pattern, and sources also positioned in a different 2-D pattern, thus causing a better illumination of the subsurface by the seismic waves. Here too,

the basic concept of adding *fold* number of traces in a CMP-gather holds sway – point-shaped CMPs and CDPs being replaced by finite *bins*, their sizes depending upon the survey design and objectives (see Vermeer 1990, 2002 for further insight into acquisition design).

In areas with structural complexity, the simplifying assumptions of CMP- processing break down, and the availability of computer power may make it possible – nay desirable – to process each trace of the recorded CSG separately, to try to obtain a better image (see also ▶ “[Seismic Imaging, Overview](#)” and ▶ “[Seismic, Migration](#)”).

Restricting the deployment to the surface of the earth implies – as we shall see later – a bias for horizontal structures; this was eventually removed by carrying out measurements inside bore-holes called VSP; see ▶ “[Vertical Seismic Profiling](#)” for details. Finally, better recording instrumentation coupled with the need to detect changes in the hydrocarbon reservoirs resulting from exploitation have given rise to *time lapse seismic* (4D), whereby repeat imaging of the same area carried out after several years of production is used to validate/improve production models for reservoirs.

Seismic Data Processing

Introduction

Reflection seismic data, acquired in the field, has to be taken through several processing steps, before it can be interpreted in terms of the subsurface structure. The source signal, on its way down, and back up to the receivers is modified by many factors; the aim of processing is to *undo* (i.e., correct for) as many/much of these effects as possible, leaving only the effects due to the causative structure of interest (geology) to be interpreted.

Seismic data is a spatio-temporal sampling of the back-scattered seismic wavefield, an ordered collection of traces, and can be considered to be a 2/3-D data matrix along with some auxiliary information regarding location, etc. As indicated before, analysis of the recorded wavefield requires it to have been uniformly and properly sampled in all relevant dimensions. Field logistics, however, frequently causes the spatial dimension(s) of the wavefield to violate this criterion. The resulting data will then be irregularly sampled in that dimension and will need resampling. Gaps may exist even within areas of otherwise equidistant traces due to problems associated with some receiver locations (houses, factories, etc.).

Interpolating the recorded data to fill up these gaps to enable further processing requires theoretical underpinnings, for example, Gülünay (2003), Zwartjes and Sacchi (2007), and Liu and Fomel (2011). These are regularly employed to preprocess the seismic data before the real work (processing) can begin. It may be mentioned here that even after recovering

uniformly sampled (spatial) wavefield obtained from an irregular acquisition geometry, the data may be aliased for coherent noise, for example, groundroll and multiples; see below for a brief explanation of these terms and ▶ “[Seismic Noise](#)” for details.

Recently there have been some interesting advances in this field, which economize by intentionally undercutting the Nyquist criterion during acquisition before recovering the wavefield by suitable preprocessing – these will be briefly mentioned at the end of this entry. Presently, the spatial dimension too will be assumed to have been uniformly- and properly sampled.

The traces themselves are an ordered collection of uniformly sampled amplitude values (*time-series*), with relevant information contained in their respective headers in (internationally) agreed formats. All processing steps aim to improve the spatio-temporal S/N ratio of the data by reducing the noise and/or by sharpening the wave-form (to improve the resolution).

Signal vs. Noise

Before proceeding further, it is useful to reflect on the terms *signal & noise*. That it is a matter of perspective is clear from this relative definition: *signal is useful noise and noise is useless signal*. In other words, someone’s noise is someone else’s signal, and vice versa. For example, the *ground-roll*, hated in reflection seismics, is useful in surface-wave seismology and shallow-seismics. Amazingly, using noise for seismic imaging has now become a field of active research (see the section “[Noise as a Seismic Source](#)” for references).

In classical reflection seismics, signal is synonymous with *primary reflection*. *Primaries*, as these are often referred to, represent seismic energy reflected only once during its travel from source to receiver. Everything else, present in the traces, is taken to be *noise*. This includes multiply-reflected energy (*multiples*), diffractions (caused by *sharp* structures in the subsurface, for example, faults, pinch-outs), refracted arrivals, surface-waves (*ground-roll*). Nongeological noise sources include nature (wind, waves, animals) and man (traffic, drilling, industry, etc.). From processing point of view, noise could be coherent (ground-roll, water-pump, multiples), or, incoherent, each needing a different strategy. See ▶ “[Seismic Noise](#)” for details.

Kinematics of the Seismic Signal (Primaries)

Starting with some simple (but inaccurate) assumptions, for example, horizontal layering, constant speed, useful structural information can be extracted – a large data volume contributing to the robustness of the processing algorithms (also see ▶ “[Seismic, Migration](#)”). In this section, we focus on the travel-times of the waves (visualized as *rays*), see also additional information in ▶ “[Seismic Ray Theory](#)”.

NMO

The travel-time for a primary-reflection from a horizontal reflector, shown earlier to be hyperbolic, can be rewritten as:

$$t_x - t_0 = \frac{\sqrt{x^2 + 4H^2} - 2H}{v}. \quad (1)$$

The quantity on the left is the difference (see Fig. 2) between the oblique reflection-time at source-receiver offset (distance) x and the vertical TWT and leads to the relation:

$$\Delta t_x = \frac{2H}{v} \left(\sqrt{1 + \frac{x^2}{4H^2}} - 1 \right) = t_0 \left(\sqrt{1 + \frac{x^2}{4H^2}} - 1 \right). \quad (2)$$

Expanding the expression under square-root, and recognizing that in most seismic measurements offset \ll target-depth, we obtain the approximate relation 3, which could be improved by retaining additional higher order terms.

$$\Delta t_x \approx \frac{x^2}{4vH} = \frac{x^2}{2v^2 t_0} \quad (3)$$

$\Delta t_x (= t_x - t_0)$ is called the *normal moveout* (NMO) associated with the reflection travel-time. NMO can be used to align the primary reflection in all traces at t_0 (TWT) by removing the effect of source-receiver distance (offset), that is, by *flattening the reflector*. NMO, an important concept in seismics, is used both to first identify *primaries* and later to align them for imaging the reflector. Note that to use 3 we need to know x (source-receiver offset), v (speed), and H (target depth); in practice, x is known and iteration is used to obtain optimal values for v and H .

Dipping Bed

For a dipping reflector (Fig. 2, below), travel-time for the primary reflection is still hyperbolic, given by

$$v^2 t_0^2 = x^2 + 4H^2 + 4Hx \sin \theta. \quad (4)$$

The minimum of the hyperbola is now shifted *updip*; the quantity $t_{+x} - t_{-x}$ is a measure of the asymmetry and can be used to estimate the dip.

Many Reflectors: Layer-Cake

Dix (1955) considered the case of many reflectors parallel to the surface – a good starting model for sedimentary sequences – and showed, that here too, the travel-time curve can be approximated at short offsets by a hyperbola:

$$t_x^2 \approx t_0^2 + \frac{x^2}{v_{rms}^2}, \text{ with } v_{rms} = \sqrt{\frac{\sum v_i^2 \Delta t_i}{\sum \Delta t_i}}. \quad (5)$$

The homogeneous velocity v ($= v_{nmo}$) is now replaced by v_{rms} (root-mean-square velocity), which depends upon the velocities of the layers v_i and the vertical transit times t_i through them. V_{rms} plays a role similar to v_{nmo} in flattening the primaries in the multilayer case. Individual layer-velocities may then be computed from the Dix' equation:

$$v_n = \sqrt{\frac{v_{rmsn}^2 t_n - v_{rmsn-1}^2 t_{n-1}}{t_n - t_{n-1}}}. \quad (6)$$

Velocities in Seismics

In seismics different terms are used to denote “velocity” depending upon the context. Table 3 lists a few, along with brief explanations, some of these will be elaborated later.

NMO Stretch

After NMO correction, a time-interval Δt_x , say corresponding to a period of the wavelet recorded on a trace at an offset x , becomes Δt_0 ; the wavelet is thus distorted (*stretched*). The expression $100 (\Delta t_0 - \Delta t_x)/\Delta t_x$ is a percentage measure of this stretch – 0% implying no distortion. In practice, a threshold percentage is specified to exclude parts of data – relatively large offsets and small arrival times – from being NMO-corrected (and taking part in further processing).

Semblance: A Measure of Signal Alignment

To apply optimal NMO correction, a quantitative measure of alignment of amplitudes, across several traces, is useful. Such a measure of similarity between n (amplitude) values, called *semblance*, is defined by

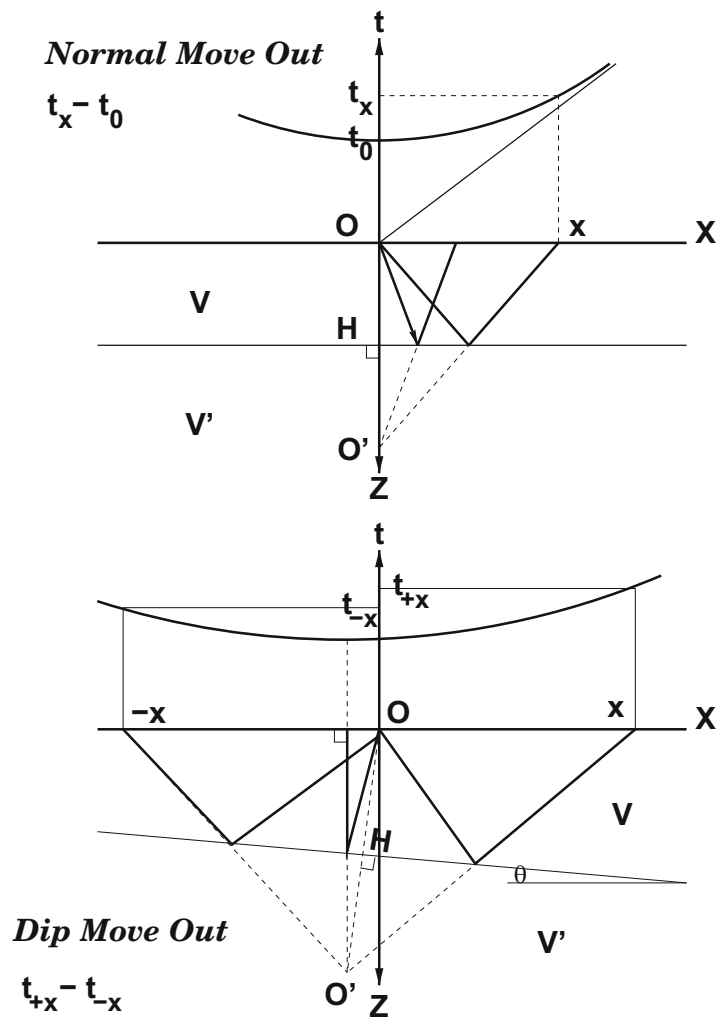
$$S = \frac{(\sum_n val)^2}{n \sum_n val^2}, \quad \text{and } S_{gate} = \frac{\sum_{gate} (\sum_n val)^2}{\sum_{gate} (\sum_n val^2)}. \quad (7)$$

Note that semblance is a dimensionless number between 1 (perfect match) and is 0 (perfect mismatch). The second form uses a time gate along the traces, generally having the width of the dominant period of the signal, for increased robustness. Semblance is used extensively in modern *reflection velocity analysis*, to evaluate the goodness of alignments of primary reflections along move-out curves computed for a range of trial velocities (Fig. 3).

Velocity: Processing Point of View

Wave-speed (called velocity in seismics) in the medium is the missing link needed to convert the travel-time information to depths required for structural interpretation – and eventually drilling. Note that *velocity* is needed to find the structure

Seismic Data Acquisition and Processing, Fig. 2 NMO of a primary reflector; horizontal (above), dipping (below). See text for details



Seismic Data Acquisition and Processing, Table 3 Jargons associated with the term velocity in seismics

Jargon	Brief description
v_{int}	Speed in a geological interval (assumed constant)
v_{av}	Average speed between two points along a ray path
v_{app}	Apparent speed measured by receivers in field ($= dx/dt$)
v_{nmo}	Speed used for NMO-correction (strictly, only for one layer)
v_{rms}	Dix' root-mean-square NMO velocity for layer-cake situation
v_{stk}	best velocity to stack CMP gathers
v_{mig}	best velocity to migrate the seismic data

(geology), but structure is needed to find the velocity. This catch-22 situation is solved iteratively – shown schematically in Fig. 4.

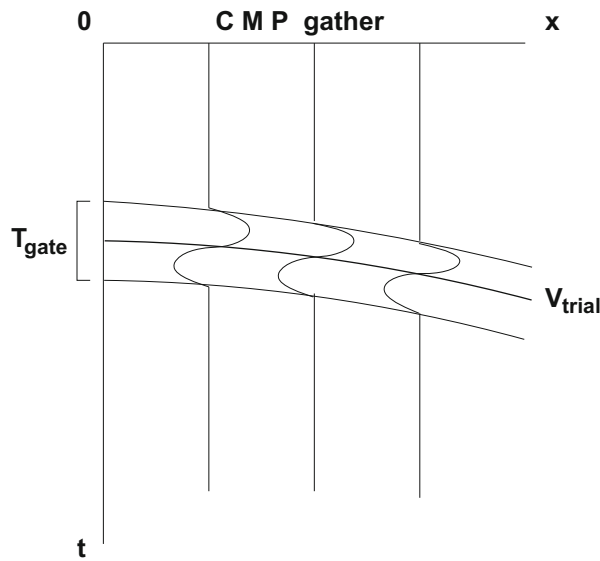
Velocity is a macroscopic (wave-length-scale average) property of the rock depending upon the density and elastic properties of the minerals making up the lithology (see ► “Seismic Properties of Rocks”). In rocks of interest in seismics (*sandstone, shale, limestone*), velocity is not a

good indicator of lithology, with considerable overlap in values, with some exceptions, for example, salt, anhydrite (relatively higher velocity). Presence of *porosity and pore-fluids (water, oil, gas)* are the most important factors for this overlap and are in turn caused by the *burial history* of the rocks. Wave-propagation in fluid-filled porous media is described by Biot-Gassman theory, see Lee (2008) for references and recent developments.

Propagation velocity (the missing link) can be estimated by direct measurements (see, e.g., Sheriff and Geldart 1995 for details), which have shortcomings though (see Table 4). The velocity used for processing seismic reflection data is usually determined iteratively from the data itself and will be described later.

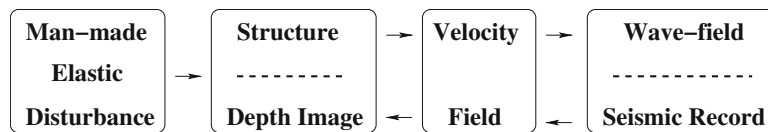
Amplitude Changes along the Propagation Path

Several factors cause the amplitude of the seismic waves to change as they travel from source to receiver. These can be corrected for, so as not to mask the weaker changes (signals) of interest.



Seismic Data Acquisition and Processing, Fig. 3 Schematic drawing showing calculation of multichannel semblance. Curved bold line represents the move-out curve for a trial velocity, and the two

surrounding lines represent the boundaries of the time-gate; see text for details



Seismic Data Acquisition and Processing, Fig. 4 Iteratively solving for both structure and velocity in seismics

Seismic Data Acquisition and Processing, Table 4 Direct determination of seismic velocities and their shortcomings

Method	Shortcoming
Uphole-time	Useful only for the weathering layer
Check-shots, well-shoot	Limited depth-range, destructive
VSP	Available late in exploration, expensive
Sonic log	Available late, noisy (high-frequency)
Lab measurements	Limited availability

Geometrical Spreading

Conservation of energy requires a continuous reduction of amplitude, as a seismic wave-front spreads through a medium – hence the term *geometrical spreading*. The loss depends upon the mode of spreading and the distance travelled (r). For primaries (body-waves), amplitude ($\propto \sqrt{\text{energy}}$) decreases $\propto r^{-1}$, whereas for ground-roll (surface-wave), the decrease is $\propto r^{-1/2}$, the latter shows why ground-rolls, with their (relatively) large amplitudes, are a big problem in seismics.

Absorption

The propagating wave continuously loses energy due to absorption too, which is a physical property of the medium,

and can be described by several equivalent parameters, for example, *absorption coefficient*, *damping factor*, the most common being the *quality factor* of the material, $Q = 2\pi/[\text{fractional energy lost per cycle}]$. It is a dimensionless quantity, with a value of 0 implying perfect absorption and ∞ implying perfect elasticity. Absorption, with Q considered to be frequency-independent within the band-width of interest in seismics, causes relatively greater attenuation of higher frequencies – leading to a change in the waveform during propagation. See ▶ “[Seismic, Viscoelastic Attenuation](#)” for more details.

Energy Partitioning at Interfaces

Boundaries of geological heterogeneities (layering, faults, etc.) also cause changes in the amplitude of the wavelet; such changes are, indeed, of prime interest in seismics. As in optics, the interaction between the wave-fronts and the geological structure depends upon their relative dimensions, that is, their radii of curvature – with specular reflections and point-scattering building the two end-members, both of which are encountered in seismics. Another concept from optics, *diffraction*, is useful to understand the complexity of the interaction between the wave-front and the medium. See

► “Seismic Diffraction”, ► “Seismic Waves, Scattering”, and ► “Energy Partitioning of Seismic Waves” for additional details.

Waveforms: Convolution, Deconvolution

Factors modifying the source signal along the path of the seismic wave may be divided as: near-source (*ns*), that is, weathering layer, earth (*e*), that is, the target geology, near-receiver (*nr*), receiver (*r*) and recorder (*rec*), with the output trace (*o*) as the final result. Each of these, denoted in Eq. 8 below by the expression in parentheses, affects (*filters*) the source wavelet (*s*). In a series of papers/reports (Robinson 2005; Treitel 2005), the MIT geophysical analysis group (GAG) laid the foundation of the *digital revolution* in seismic data processing, by examining the nature of these filters and developing methods to undo their effects. These resulted in major advances in *time-series analysis and digital filtering* (Robinson and Treitel 1964) and a critical evaluation of the (statistical) nature of earth’s reflectivity (*target geology*).

Convolutional Model of the Seismic Trace

As the source – and recorded – signals are both time-series (uniformly sampled, ordered collection of amplitudes), it is useful to represent all the other elements mentioned in the above-paragraph also as such. For a column of vertically layered reflectivity, such a time series would correspond to values equal to RCs placed at times converted from depths using velocities. Now, making the crucial assumption that all these filter elements are linear systems, the recorded trace can be expressed as:

$$o(t) = s(t) * ns(t) * e(t) * nr(t) * r(t) * rec(t) + n(t). \quad (8)$$

In Eq. 8, $*$ (*star*) is the convolution operator, well-known in the theory of linear systems; $n(t)$ represents some additive noise which does not follow this model, hopefully, it is mostly removed early in the processing. The time-series that transform $s(t)$ into $o(t)$ can also be interpreted as the *impulse response* of the corresponding elements, for example, $r(t)$ is the response of the receiver to a sudden spike signal. Using *Fourier-Transforms* to change the time-series into their *spectra*, and remembering that convolution in time-domain corresponds to multiplication in frequency domain, one obtains:

$$O(\omega) = S(\omega) \cdot NS(\omega) \cdot E(\omega) \cdot NR(\omega) \cdot R(\omega) \cdot REC(\omega), \quad (9)$$

where the noise term has been neglected (see Sheriff and Geldart 1995 for introduction to linear operators and Fourier theory). Equation 9 clearly shows the *filtering* effect of the different elements, each one modifying the spectrum of the incoming signal by modifying/removing a part of its

frequencies. Our aim, in seismic data processing, is to extract $e(t)$, the geological structure from the recorded signal $o(t)$.

Deconvolution as Inverse Filtering

Undoing the act of the filterings implied in Eqs. 8 and 9 is called *deconvolution* (decon), or, *inverse filtering*. Equation 9 can be rewritten as $O(\omega) = E(\omega) \cdot REST(\omega)$, where $REST(\omega)$ groups together all the elements on the right besides the geology. Then, $E(\omega)$, or $e(t)$, can be *estimated* from

$$\begin{aligned} E(\omega) &\cong O(\omega)/REST(\omega), & \text{or,} \\ e(t) &\cong o(t) * rest(t)^{-1}. \end{aligned} \quad (10)$$

The approximation sign, for both forms of Eq. 10 – in frequency-domain (first), or, in time-domain (second) – is necessary, even in the *noise-free* case. Spectral division needs precautions to avoid zero-division in parts of the spectrum, where frequencies have been weakened/removed. Fortunately, addition of *noise* helps, since signals of interest in seismics exist – by definition – only above the ambient noise level. See Liner (2004), Sheriff and Geldart (1995) and Yilmaz (2001) for the stabilizing role of *spectral whitening* in decon.

Wavelet Processing

Wavelets: Let’s take a closer look at *seismic wavelet*, introduced in the section about “Seismic Sources,” as a signal of finite frequency band-width and temporal duration. Using standard concepts from time-series analysis (Sheriff and Geldart 1995; Yilmaz 2001), simple examples of wavelets are:

$$a : (3, -2, 1), \quad b : (2, 3, -1) \quad \text{and} \quad c : (-1, 2, 3),$$

the numbers representing uniformly sampled amplitudes starting from $t = 0$. Remembering that squares of the amplitudes in a wave(let) are measures of energy, we see that these three wavelets, while looking very different, have the same total energy. Depending upon the energy build-up, wavelet a is called *minimum-delay* (energy is front loaded), b is *mixed-delay*, and c is *maximum delay*; physical (causal) wavelets are minimum delay, although in the example, a is not strictly causal, due to the instantaneous build-up of energy at $t = 0$. In frequency domain, the expressions minimum/mixed/maximum-phase are used instead.

Wavelet estimation: *Auto-correlation* of the wavelets a-c are all symmetrical about $t = 0$, that is, have no phase information, for example, $\varphi_{bb} = (-2, 3, 14, 3, -2)$; these are Fourier Transforms of the respective power-spectra. In seismics, an estimate of the power spectrum is often available from the data. The question then arises whether an estimate of the wavelet may be obtained from it – an outline follows.

Using Z-transform notation, one can write the wavelet, say c , and its auto-correlation as polynomials:

$$C(Z) = -1 + 2Z + 3Z^2, \text{ and,} \\ \Phi_{cc}(Z) = -3Z^{-2} + 4Z^{-1} + 14 + 4Z - 3Z^2,$$

Z being the *unit-delay* operator, its powers denoting time-shifts with respect to $t = 0$. According to the fundamental theorem of algebra, a polynomial of degree n in Z must have n roots, that is, it can be expressed as a product of n factors of the form: $(Z - Z_1)(Z - Z_2) \dots (Z - Z_n)$, each factor representing a basic wavelet (*doublet*). Half the doublets of an auto-correlation polynomial are minimum-delay; their product represents the Z-transform of the unique minimum-delay causative wavelet. See Yilmaz (2001) and Sheriff and Geldart (1995) for details, assumptions, critical remarks, and alternate approaches (e.g., *homomorphic deconvolution*) to deconvolution of time-series.

Wavelet manipulation: Much of seismic processing is involved with manipulating the wavelet (deconvolution in a general sense). While very powerful, it contains potential for pitfalls, if applied without a proper understanding of the suitability of the particular technique, as each decon step also causes artifacts.

Spiking decon aims to sharpen the shape of the signal, to improve temporal resolution – and interpretation. Ideally, it involves convolving the wavelet with its inverse operator, to yield a spike, that is, perfect resolution.

Zero-phasing converts the signal to one with zero-phase; the result is a symmetrical signal (a-causal) and is primarily useful for interpretation if the peak can be made to coincide with the reflecting boundary.

Any-phasing is used in merging seismic datasets of different vintages and with differing source wavelets.

General shaping groups methods to convert the signal to any desired shape optimally – using some statistical criteria.

Depending upon whether a model is available for decon, the methods could also be divided in *deterministic*, that is, model-based and *statistical*.

Deterministic Deconvolution

Vibrois processing: Vibrators (see the section on “[Seismic Sources](#)”) use a repeatable source signal, called *sweep*. It is a time-limited (typically, 10–20s long) signal with the frequency continuously varying between given start- and end-values and comes in many flavors, for example, up-, down-, linear-, nonlinear-sweeps. Neglecting other terms, one could write from Eqs. 8 and 9: $o(t) = s(t) * e(t)$. The recorded signal is thus the convolution of *earth reflectivity* with the sweep signal. We could remove its effect (deconvolve) by *cross-correlating* the observed signal with the sweep (which we

know precisely), a process, which is equivalent to convolving with its time-reversed version, and get

$$s(-t) * o(t) = s(-t) * s(t) * e(t) \approx \delta(t) * e(t) \approx e(t). \quad (11)$$

Due to the sweep-signal being time-limited, its auto-correlation is not a Delta-spike (ideal), but is a symmetrical (zero-phase) signal called *Klauder wavelet*. The result is thus not quite the desired earth reflectivity (although it has the correct phase) and needs further processing for improvement (see Yilmaz 2001; Liner 2004; Sheriff and Geldart 1995).

De-ghosting: The effect of large RC s in the shallow sub-surface has been mentioned earlier. Figure 5 (above) shows one such situation; here the source is placed below the weathering layer, for better energy transmission towards the deeper target (ray going directly downwards). A part of the wave-energy also travels upwards and gets reflected down from the base of the weathering layer (ray going first up, and then down). In certain cases, the $RC_{weathering}$ could be quite large and negative. The energy reflected downwards follows with a short delay behind the direct wave and is called a *ghost*; the observed record is thus corrupted by that caused by a delayed ghost. Removing the latter from the recorded trace is called *deghosting* and is an example of model-based decon. Assuming the TWT between the source and the base of the weathering to be n samples ($= n\Delta t$), one can write: $o(t) = s(t) - Rs(t - n\Delta t)$, or, using Z-transforms,

$$O(Z) = S(Z) - RS(Z) \quad Z^n = S(Z)(1 - RZ^n).$$

$(1 - RZ^n)$ is, clearly, the Z-transform of the ghost-operator. Hence,

$$S(Z) = R(Z)(1 - RZ^n)^{-1}, \text{ or, } s(t) = o(t) + s(t - n).$$

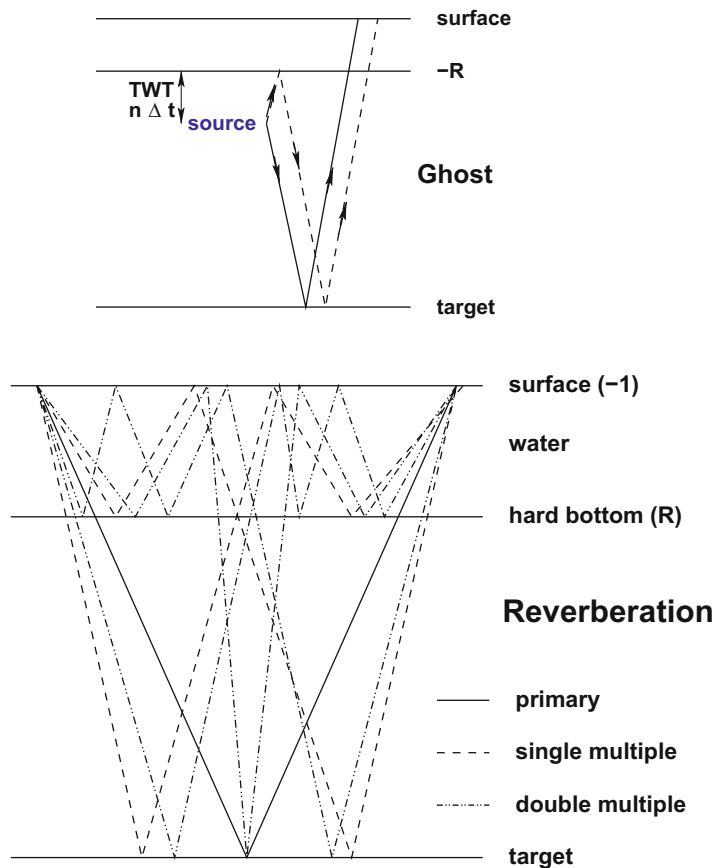
The last form above implies recursive filtering in the time-domain to achieve deghosting. Alternately, expanding $(1 - RZ^n)^{-1}$, the inverse-filter operator in time-domain can be written as

$$g(t)^{-1} = (1, 0, 0, \dots + R, 0, 0, \dots + R^2, 0, 0, \dots)$$

De-reverberation The lower part of Fig. 5 shows another situation, where strong reflectivity associated with the water-bottom causes long trains of high-amplitude *reverberation* of signals in the water-layer. The ray-paths shown schematically are: one primary reflection from the target, *two* multiples reflected once in the water layer, and *three* multiples reflected twice; there could be many more, posing a serious problem in marine seismics. Depending upon the

Seismic Data Acquisition and Processing, Fig. 5

deterministic deconvolution applied to ghost (above) and reverberation (below). The near vertical ray-paths are shown obliquely for better visualization, see text for details



depth of water, certain frequencies will, as a result, experience severe distortion (enhancement or suppression). In the simplified case of a water-column with a TWT equal to the sampling interval, and remembering that the negative reflectivity causes phase-change, the total operator (signal + reverberation) can be written as:

$$w(t) = (1, -2R, +3R \dots) \rightarrow W(Z) = 1 - 2RZ + 3R^2Z^2 - \dots = (1 + RZ)^{-2}.$$

It follows that the deconvolution in this case can be achieved by the operator

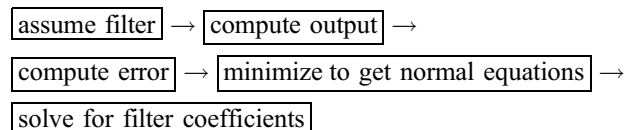
$$W(Z)^{-1} = (1 + RZ)^2, \text{ or, } w(t)^{-1} = (1, 2R, R^2).$$

This elegant operator is called the Backus filter (see Backus 1959).

Statistical Deconvolution

In the absence of a deterministic model, one could attempt to change the signal wavelet to any desired shape, by designing filters that are optimal in a statistical sense. Based upon work in information theory by Norbert Wiener and others, the applications in seismics were pioneered by the MIT-GAG

group, for example, Robinson (1967). Schematically, the basic approach is:



If errors are assumed to be Gaussian, and l_2 norms are used, the operators obtained are called Wiener filters. Such *optimum filters* are used widely, for example, in

- Zero-lag spiking – to increase resolution
- Zero-phasing – to ease interpretation
- Prediction Filtering – to remove multiples which are predictable, the remnant being the prediction error, corresponding to the deeper signal

Wiener optimum filter The normal equations for the filter-coefficients f are given by the matrix equation shown in Eq. 12 in its compact form

$$\phi_{input,input} * f = \phi_{input,output}, \quad (12)$$

which relates the auto-correlation of the recorded (*input*) wavelet to its cross-correlation with the desired (*output*) wavelet. For the derivation of Eq. 12, and a detailed treatment of statistical deconvolution, see, for example, Yilmaz (2001) or Sheriff and Geldart (1995) – an example is shown below to illustrate the approach.

Spiking filter If the wavelets are all n -sample long, the Matrix Eq. 12 can be expanded as

$$\begin{pmatrix} \phi_{i,i}(0) & \phi_{i,i}(1) & \dots & \phi_{i,i}(n-1) \\ \phi_{i,i}(1) & \phi_{i,i}(0) & \dots & \phi_{i,i}(n-2) \\ \phi_{i,i}(n-1) & \phi_{i,i}(n-2) & \dots & \phi_{i,i}(0) \end{pmatrix} \begin{pmatrix} f_0 \\ f_1 \\ \dots \\ f_{n-1} \end{pmatrix} = \begin{pmatrix} \phi_{i,d}(0) \\ \phi_{i,d}(1) \\ \dots \\ \phi_{i,d}(n-1) \end{pmatrix} \quad (13)$$

The auto-correlation matrix $\phi_{i,i}$ in Eq. 12, with the same element in each diagonal descending from left to right, is a Toeplitz matrix; f is a column vector with the filter-coefficients to be determined and $\phi_{i,o}$ is a column-vector with elements from the cross-correlation matrix. Equations with Toeplitz matrices can be efficiently solved by a procedure called *Levinson recursion*.

Wiener filter: a simple example Given the input wavelet $i_t = (1, -1/2)$, let us find the optimum two-element Wiener-operator to transform it to the desired wavelet $d_t = (1, 0)$, that is, a zero-delay unit-spike. We get, $\varphi_{i,i} = (5/4, -1/2)$, and, $\varphi_{i,d} = (1, 0)$. Equation 13 then becomes

$$\begin{pmatrix} 5/4 & -1/2 \\ -1/2 & 5/4 \end{pmatrix} \begin{pmatrix} f_0 \\ f_1 \end{pmatrix} = \begin{pmatrix} 1 \\ 0 \end{pmatrix},$$

yielding $f_{Wiener} = \left(\frac{20}{21}, \frac{20}{21}\right)$.

Applying this filter to the input, we obtain the output $(20/21, -2/21, -4/21)$, which compared to the desired output, gives a squared-error of $1/21$. The ideal filter for this decon is the *inverse filter* for the input wavelet. Writing $I(Z) = 1 - Z/2$ for the Z -transform of the input, the Z -transform of the inverse-filter (which will convert the input to an ideal unit-spike) is $(1 - Z/2)^{-1} = 1 + Z/2 + Z^2/4 + \dots$, which is an infinitely long operator! For an honest comparison of its performance with that of the Wiener-filter, we apply its first two terms to the input, getting the filtered version as $(1, 0, -1/4)$; although looking better at the first

Seismic Data Acquisition and Processing, Table 5 Performance of Wiener- and Inverse-filters

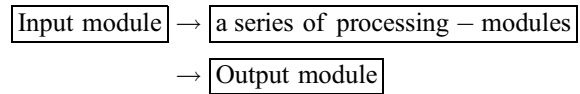
Input wavelet	Desired wavelet	2-point Wiener		2-point inverse	
		Filter	Error	Filter	Error
(1, -0.5)	(1, 0)	(20/21, 8/21)	1/21	(1, 0.5)	1/16
(-1/2, 1)	(1, 0)	(-10/21, -4/21)	6/21	(-2, -4)	16
(-1/2, 1)	(0, 1)	(16/21, -2/21)	4/21		

glance, its squared error is $1/16$, that is, larger than that of the Wiener-filter! It can be shown that the Wiener filter is the *best* two-element filter for this problem.

Suppose the input wavelet is $(-1/2, 1)$, that is, not minimum delay, which we want to transform to a zero-delay spike. Normal equations now give the Wiener-filter as $(-10/21, -4/21)$, with the output $(5/21, -8/21, -4/21)$ and the squared error as $6/21$. Inverse filter is now $(-2, -4, -8, \dots)$, which is extremely unstable! Its first two filter-elements give the output $(1, 0, -4)$ with 16 as error! Wiener filter performs here worse than in the first case, because it was trying to convert a maximum-delay wavelet to a minimum-delay spike, but it still does better than the (finite) inverse filter. In this case, if a maximum delay spike $(0, 1)$ was desired, Wiener-filter coefficients would be $(16/21, -2/21)$, giving a filtered output of $(-8/21, 17/21, -2/21)$ with a squared error $4/21$, which is better than that for a zero-lag spike output. Table 5 summarizes the results.

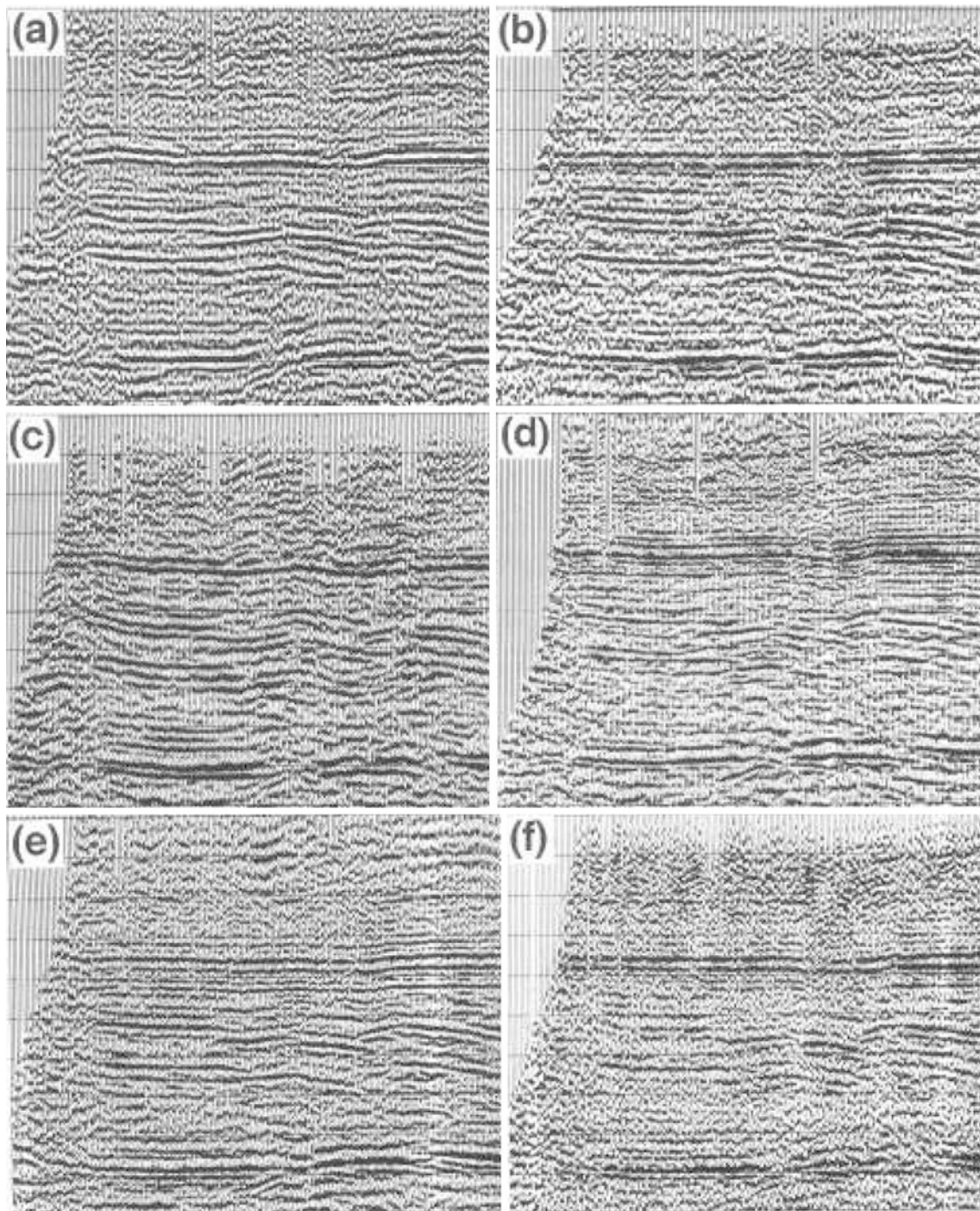
The Processing Flow: Putting it all Together

Most of the processing *modules (filters)* operate on the data (time-series) sequentially, the entire process resembling a *flow*, though there are a few stand-alone modules too. The operations could be on individual traces (*single-channel*), or on a gather of traces (*multichannel*). Schematically, a seismic processing flow looks like:



Modules have been developed for carrying out specific tasks within the flow, for example, static correction, band-pass filtering, stacking, migration. Usually, there is a choice of modules (algorithms) available for a specific step – each with slightly different characteristics (and artifacts) – and the proper selection of the modules for a flow needs both expertise and experience. This point is illustrated in the Fig. 6, which shows six *different* results of processing the same data.

An overview of commonly applied *corrections* (processing module) is shown in Fig. 7. Space constraints will permit us to briefly describe only selected items from this list, which itself is not exhaustive; see Yilmaz (2001) for a more detailed treatment, and ► “[Seismic Imaging, Overview](#)”



Seismic Data Acquisition and Processing, Fig. 6 Seismic Data Processing has no perfect answer. Seismic cross-sections produced from the same data processed by six different contractors. (Figure from Yilmaz 2001, courtesy SEG and the author)

for additional information. Note that some modules may be applied more than once in the flow, and also, that parts of the flow may be iteratively repeated, till a reasonable result is obtained. The latter shows the importance of quality control (Q/C), by means of visual-display and other (quantitative) tools. The decision as to whether the processing of a dataset is finished depends often on the geological objectives,

technical possibilities, and managerial constraints of time and money.

Preprocessing

Editing of seismic traces is an important first step, in view of the largely automated processing sequences later. *Geometry assignment* is also an essential step at this stage and attaches

Seismic Data Acquisition and Processing, Fig. 7

Components of seismic processing flow

Pre-processing

QC: edit bad traces – assign field-geometry – resample – notch-filter

Pre-stack processing

statics: elevation – datum – residual

amplitude: spreading – Q-compensation – mute – balance

filtering: band-pass – f-k – f-x – τ -p – median – notch

deconvolution: deterministic – predictive – statistical

velocity analysis: CMP sort – const. velocity stack – semblance analysis

stack: NMO correction – DMO correction – CMP stack – AGC – display

Post-stack processing

migration velocity analysis – migration – time-to-depth – display

No-stack processing

migration velocity analysis – prestack depth migration – display

Special processing

True Amplitude (AVO, DHI) – VSP – Anisotropy – image rays

acquisition information to the traces, for example, source- and receiver-coordinates. Each seismic trace is assigned a header, to store such and other information to enable efficient inter-process communication.

Prestack Processing

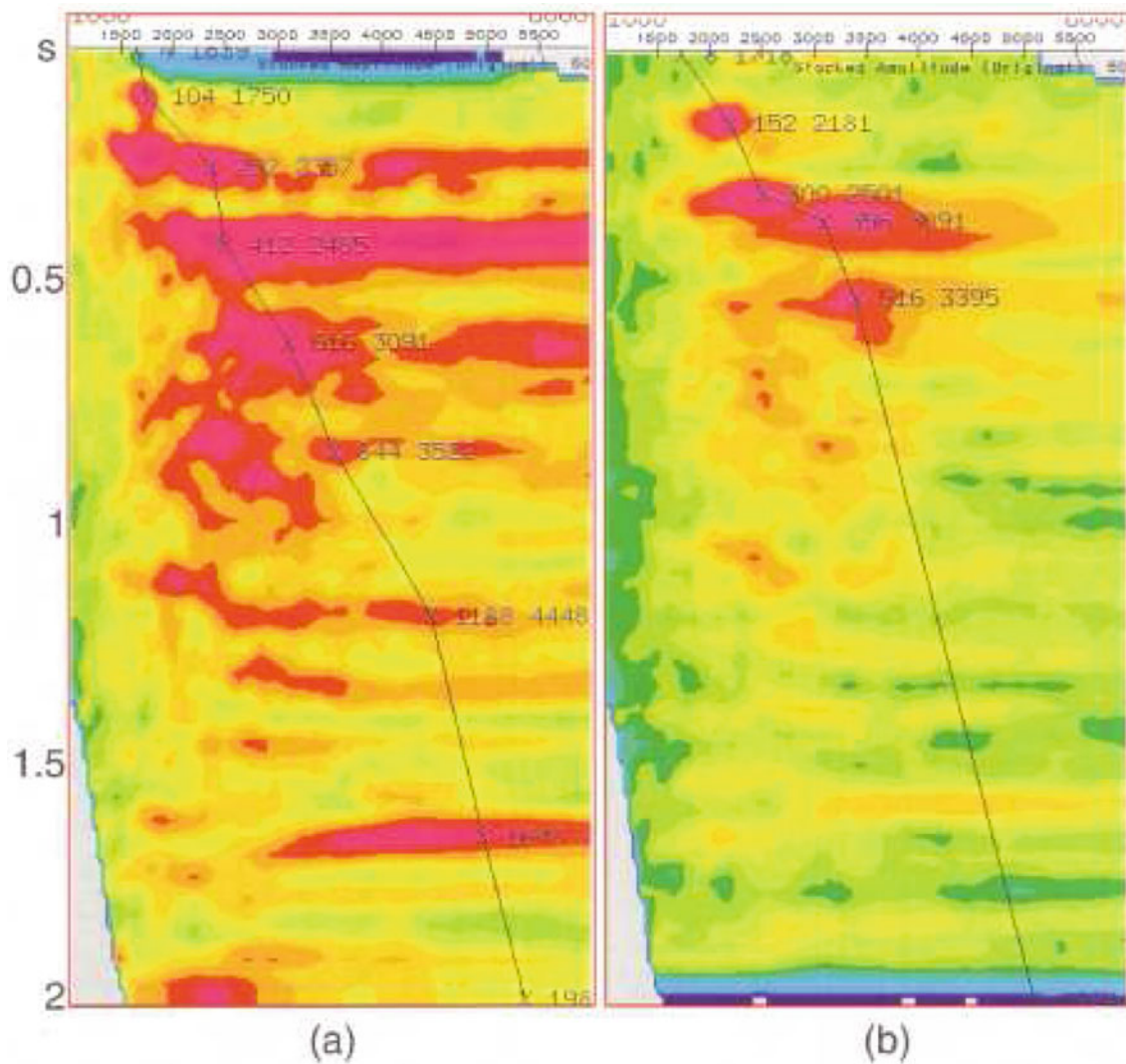
Static corrections These are time-invariant corrections applied to the traces, due to, for example, elevation differences, and involve up-, or, down-shifting the entire trace in time; an example of their dramatic effect can be seen in Fig. 8. The static effects due to slow lateral changes (long wavelength statics) are particularly difficult to model and can cause imaging problems. *Residual statics* involves *small* time-shifts applied late in the flow to improve the result; it uses the powerful concept of *surface-consistency* to try to correct for near-surface errors that were not modeled properly in the earlier stages. Its implementation by Rothman (1985) heralded the use of nonlinear optimization (*simulated annealing, genetic algorithm*) in seismics.

Amplitude corrections Loss of amplitude due to *geometrical spreading* and *absorption* can be corrected for using the theory described earlier; the latter needs a Q-model, in the absence of which empirical relationships based on the total

travel path/time are used. A part of the record may be removed from processing due to the presence of noise, or suspected nonprimaries; depending upon the part of the data-volume removed, one then talks about *top-mute*, *bottom-mute*, or a *generalized mute*. Similarly, a *balancing* (amplitude equalization) may be applied to several adjacent traces to compensate, in an ad hoc manner, for local variations, for example, bad receiver coupling.

Filtering, sharpness, taper Any process that removes/reduces a part of the suspected *noise* from the data is a *filter*. Frequency-filters (high-cut, low-cut, band-pass) are the simplest examples. Data $f(t)$ is transformed using Fourier theory to its spectrum $F(\omega) = A(\omega) \exp^{-i\omega t}$ in the frequency domain, the amplitudes mainly corresponding to noise are zeroed-out, and the data is transformed back to the time-domain. Development of algorithms for fast and efficient Fourier transform of time-series (FFT) have caused large scale application of digital filters.

Multichannel data enables double-transformation of $f(x, t)$ to $F(\omega, k)$, making filtering possible based upon slopes (apparent velocities) in the ω - k plane; this is particularly effective in eliminating, for example, slow travelling ground-roll (large amplitude surface waves), which often



Seismic Data Acquisition and Processing, Fig. 8 Stacking velocity analysis using semblance (color contours). Semblance values are shown for a dataset for a range of trial velocities (horizontal- axis) and enable interactive velocity picking as a function of TWT (vertical- axis). The

right panel shows a dramatic improvement in resolution as a result of proper static correction. (Figure from Yilmaz 2001, courtesy SEG and the author)

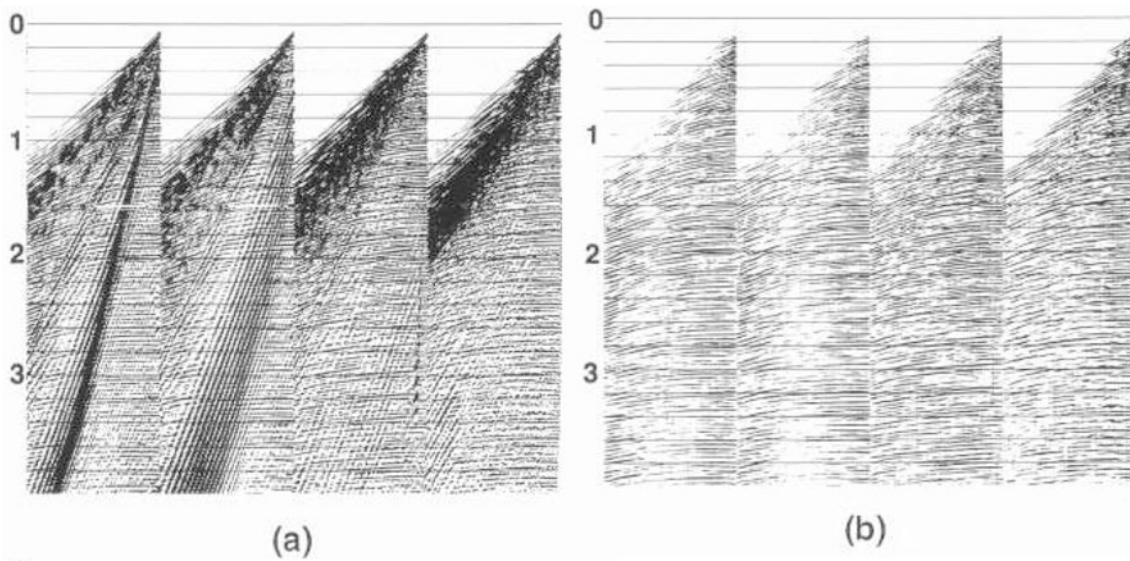
mask the primaries. An example of such filtering is shown in Fig. 9. *Notch* filters are used to remove a narrow band of frequencies, for example, a 50 Hz noise from overhead transmission line. τ - p transforms are useful in filtering multiples, and in untangling far-offset data for velocity analysis, these use the Radon domain for the decomposition (Phinney et al. 1981). A few general comments apply to all filters:

- Filtering is effective only to the extent of signal-noise separation in the transformed domain.
- For any filtering, there is a trade-off between sharp cut-offs in the transform- domain and oscillatory artifacts in time-domain – and vice versa. A compromise solution to this

unavoidable problem is to apply *tapers* to smoothen the cut-off and thus minimize edge-effects.

Deconvolution This important aspect has been dealt with in some detail in an earlier section.

Stacking velocity analysis This is almost always carried out in the CMP-domain, after *re-sorting* the data. The aim is to determine the velocity model, that is, $v_{rms}(TWT)$, to be used for computing the best move-out correction for the CMP-gathers. For a suite of velocity models, hyperbolic move-out curves are computed for the range of TWTs of interest; semblances are then computed to determine how well the arrivals in the gather line-up along these curves and displayed in a contour plot in the v_{trial} -TWT domain, allowing interactive picking of an improved velocity model (Fig. 8). The



Seismic Data Acquisition and Processing, Fig. 9 Use of two-dimensional Fourier Transform as an apparent-velocity filter for four marine-seismic records brings out (weaker) reflections. (Figure from Yilmaz 2001, courtesy SEG and the author)

process is repeated at as many CMPs as possible – sometimes grouping neighboring CMPs together for averaging, velocity being a macroscopic property. The result is a laterally varying model of v_{rms} . Equation (6) can now be used to infer interval velocities.

CMP-stack Once a reasonable velocity function has been determined, each trace in the CMP-gather (say, CMP_4 in Fig. 1) is shifted in time by subtracting the corresponding move-out corrections. The move-out corrected traces in the CMP-gather are then added (*stacked*) together to produce one trace. This process, *CMP-stack*, reduces random noise – which does not line-up, while strengthening the reflection signal – which does, and thus improves S/N ratio of the data. Note that stacking reduces the data volume too – by a factor of *fold*! Much of the power of the seismic imaging derives from this simple step, which enhances the *primary* reflections (those only once reflected) at the expense of everything else.

Zero-offset traces/sections The stack traces are also called *zero-offset* traces, the move-out correction having made the source and receiver coincident. A collection of stack traces is a stack- or zero-offset section and represents the first (albeit approximate) 2-D cross-section of the subsurface. For display purposes, CMP-stack sections may be subjected to *automatic gain control* (AGC), an extremely nonlinear time-variant amplitude scaling, to balance weaker/deeper signals and stronger/shallower ones.

Poststack Processing: Positioning Properly

The CMP-stack has one big drawback, and dips were neglected throughout, which is what we are really after. This

results in many artifacts in the section, for example, crossing layering, diffraction tails. Anticlinal structures are somewhat flattened, and synclinal structures could give rise to *bow-ties*.

Migration Fig. 10 shows the problem schematically in the CMP-domain, for the case of a trace recorded from source S at receiver R from a reflector with a dip θ . After conventional prestack processing, the zero-offset trace would be plotted on the t axis below the mid-point M . This is clearly an error, as the zero-offset ray for M should be incident normally on the reflector – at N , this correction is called *migration* (Yilmaz 2001; Sheriff and Geldart 1995).

Migration steepens and shortens energy alignments and moves these up-dip, clarifying the tangled image. Figure 11 shows an example of a successful migration. For further details, please see ▶ “Seismic, Migration”.

DMO Fig. 10 shows yet another error to be considered – the actual reflection point for the source-receiver combination $S-R$ is P , and not N . Even worse, for the different $S-R$ pairs making-up the CMP-gather with mid-point M , the reflection points are all different, that is, are *smear*ed along the reflector, the amount of smear being dip-dependent. The process used to correct for this dip-dependent part of the move-out correction is called *DMO*. In practice, this step is applied before migration as indicated in Fig. 7; Figure 10 shows the sequence:

- Reflection time is NMO corrected and plotted *below* M .
- NMO corrected time is DMO corrected and plotted below M' , the *true* zero-offset point.

- NMO + DMO corrected time is MIGRATED and plotted at P, the *reflection point*.

Time-to-depth conversion For final structural interpretation, the TWTs in the seismic section (stacked, or, migrated) need to be converted to depths, with velocity again playing the key role. For a homogeneous medium, this is just a rescaling of the vertical axis; with the velocity varying smoothly only in vertical direction (e.g., for flat sedimentary sequences), a non-uniform stretch of the vertical axis may suffice. Laterally varying velocities present depth-conversion problems though, increasing with the strength of the heterogeneity; ray-bending now needs to be taken into consideration.

No-Stack Processing: Imaging Complex Structures

In the presence of strong lateral velocity variations (e.g., below salt structures), the conceptual model used to process CMP-gathers breaks down. Removing the simplifying

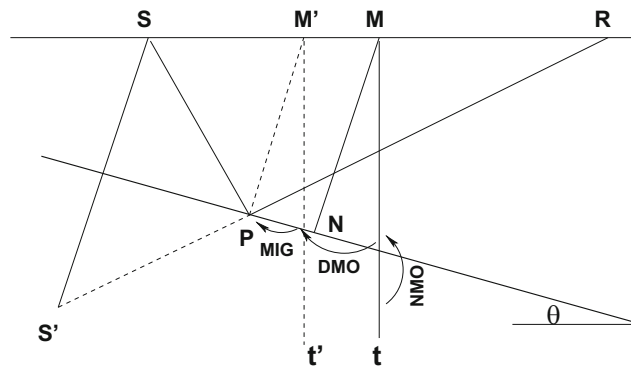
assumptions makes the imaging physically more reasonable, albeit at the cost of substantially increased computational effort.

Prestack depth migration and Migration velocity analysis

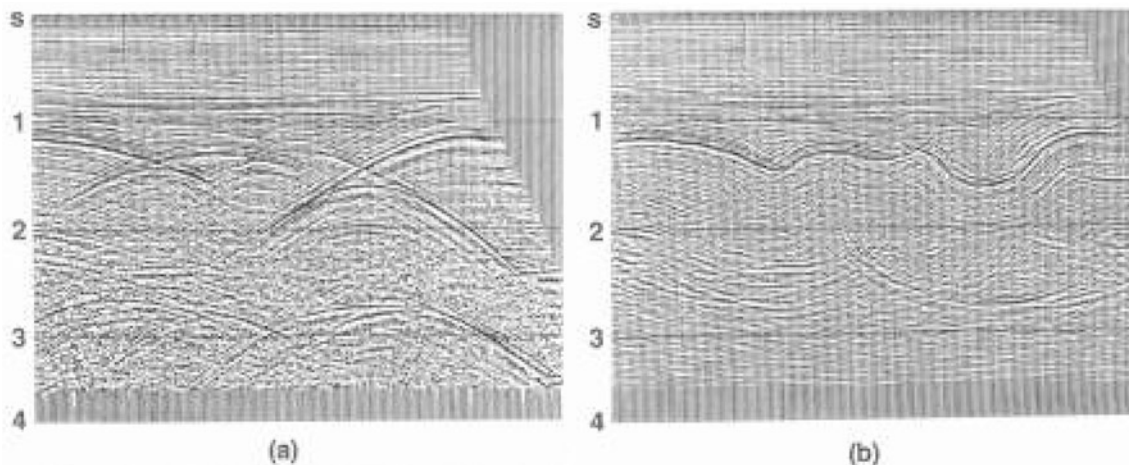
Simply put, *prestack depth migration* involves tracing the seismic energy from the source to the receiver for every recorded trace, with the philosophy that every seismic trace should be computable *if the structure and the velocity model were both known*. A detailed velocity model is essential for the success of PSDM; often a simplified model is assumed and iteratively improved using *migration velocity analysis* (MVA). For details/issues regarding 2-D vs. 3-D, time- vs. depth- and post-stack vs. prestack migration, see ► “[Seismic, Migration](#)” and Yilmaz (2001).

Special Processing

True amplitude – AVO, DHI Observed variations of the *RC* with respect to angle of incidence may be interpreted in terms



Seismic Data Acquisition and Processing, Fig. 10 Effect of dip in positioning the reflector



Seismic Data Acquisition and Processing, Fig. 11 Migration positions energy from dipping structures properly. Here bow-tie like artifacts in the top part of panel (a) are imaged back into causative synclinal

structures in panel (b). The artifacts persisting in the bottom of panel (b) probably point to lack of interest in imaging deeper structures in this case. (Figure from Yilmaz 2001, courtesy SEG and the author)

of changes in lithology across the reflecting boundary (*amplitude* versus *offset*, or, *AVO*) and may even indicate the nature of the pore-fluids. Such *direct hydrocarbon indicators* (DHI) include *bright-spots*, *flat-spots*, *polarity-reversals*, etc. (see Yilmaz 2001; Sheriff and Geldart 1995). A prerequisite for such analyses is *true amplitude processing*, avoiding modules that remove differential amplitude information, for example, balancing, stacking, AGC.

Converted waves Using multicomponent receivers, it is possible to identify waves that have been converted at the reflection boundary and hence possess asymmetrical up- and down-ray-paths. Proper processing of such data, with CCP (*common conversion point*) replacing CDP, provides a better constraint for imaging.

VSP & Cross-well tomography Bore-holes can be used for placing receivers (and sources), resulting in significant noise-reduction. The first processing step now is to separate up- and down-going wavefields, for details, see ► [“Vertical Seismic Profiling”](#).

Anisotropy Many seismic media are *anisotropic*, a common example being shales, which exhibit faster speeds parallel to the layering than across it, and require modification of procedures for proper imaging, for example, the move-out curve would no more be hyperbolic. This field is proving important for reservoir studies too, see Helbig and Thomsen (2005) for an overview and also ► [“Seismic Anisotropy”](#).

Some Recent Developments

Recording overlapping wavefields Several efforts have been initiated recently to gather more (denser) data without significantly adding to the recording time. Commonly referred to as *simultaneous/continuous sources*, these use rapidly firing sources, for example, airguns/vibrators in marine surveys, and record wavefields overlapping in time (*blending*), which are later separated using various flavors of *deblending*. This results in a considerable increase in spatial bandwidth due to much closer spacing of the sources. Not having to repeatedly reshoot the lines later from the intermediate source locations also leads to significant savings of time (read: *costs*) besides improving data quality by reducing/eliminating unavoidable location errors. Another variation of this approach is “simultaneously” recording sources from different azimuths for both land- and marine-surveys.

Blending/deblending in seismic acquisition mentioned above involves coding/decoding different parts of the recorded wavefield in a manner enabling their later separation. The subject is well known in communications theory; the “Cocktail Party Effect” uses differential characteristics of the desired signal (voice of a single person at a distance) to make it understandable from out of a cacophony of many others including some (loud) near ones (Cherry (1953)).

The related but different issue of intentionally recording overlapping signals in seismics is not new (Garotta 1983), although it is currently undergoing rapid development – both in theoretical and practical aspects (Beasley 2008). Carrying the idea farther, an interesting case has been reported, wherein wavefields generated by individual elements of the airgun firing at rapid but randomized intervals are being continually recorded (Hegna et al. 2019).

Simultaneous sources could be a game changer in the field of seismics due to its positive impact on several fronts – faster, cheaper, safer, and better, for example, Nakayama et al. (2019).

Randomly undersampling the wavefield The importance of properly sampling the seismic wavefield in both temporal and spatial dimensions has been stressed before, as the first step for deriving accurate structural information regarding the subsurface. Sampling in the time domain is usually not a problem albeit at the cost of the increased data volume (by the factor) associated with oversampling with respect to the Nyquist criterion.

Proper sampling in the spatial domain à la Nyquist, however, is a different story and is seldom achieved in a modern acquisition setting, owing partly to the scale of operations – the necessary preprocessing step of interpolation of traces to fill-up the “gaps” has already been mentioned.

The necessity – or otherwise – to adhere to the Nyquist criterion while sampling analog signals has been studied also by signal processing engineers. Recent work in information theory has shown that signals can indeed be recovered even from (severely) undersampled data under certain circumstances. If the signal of interest exhibits a certain structure in a transformed domain, it can be sampled below the Nyquist criterion and recovered in that domain – fortunately, this characteristic is shown by reflection seismic data too.

One of the earliest contributions in this field, specifically for the case of spatial undersampling in reflection seismics, was by Bednar (1996). In it, the possibility of *randomly* sampling the wavefield spatially was discussed and was hinted to be more efficient and economical than uniform undersampling. This is perhaps not surprising, given that imaging reflectors is essentially summing up (integration) of energy along certain specified trajectories (see ► [“Seismic, Migration”](#)), and efficient evaluation of integrals by summing values at random points is known in applied mathematics.

In practice, *random* undersampling of the signal is supposed to perform superior to *regular* undersampling as it will convert *aliased* energy (due to undersampling) into incoherent noise, which can then be easily filtered out. Hennenfent and Herrmann (2008) showed *jittery* undersampling (with respect to the Nyquist criterion) to perform even better, as it also enables control of the omnipresent gaps that need to be filled by interpolation for later reconstruction. Herrmann (2010) discusses this idea of randomized undersampling further. Developed from the technique of *compressive sampling*,

commonly used in modern electronics, e.g., digital camera and magnetic resonance imaging, it is shown to lead to a significant reduction in data volume and hence to be able to master the “curse of dimensionality” – a phrase which points to the exponential increase in data volume with each added dimension of seismic acquisition. It is again shown to be particularly effective, if the signal is sparse in a suitable transform-domain.

Further studies about the applicability of this technique to related fields, for example, ▶ “[Seismic, Waveform Modeling, and Tomography](#)” are subjects of active current research. One may dare to state that the Nyquist sampling criterion has at last been conquered – at least as far as seismics is concerned!

Noise as a seismic source As hinted in the first edition, it is now an exciting and established field of research under the general banner of *seismic interferometry & daylight imaging*. Starting from early conjectures (Claerbout 1968) and later breakthroughs (Fink 1993, 1997), there have been both theoretical and practical advances understanding its possibilities and limits. Although this topic belongs to some other essays in this volume (▶ “[Seismic, Ambient Noise Correlation](#)”, ▶ “[Seismic Noise](#)”), a very brief introduction follows. The basic idea is that “noise” – also in seismics – contains useful information, which can be extracted by – and this is somewhat surprising – some pretty straightforward processing. Noise recorded at two locations can be used to obtain relevant medium properties in the intervening medium. This approach can also be used to place virtual sources anywhere in the medium. For an introduction to this fascinating subject, see Curtis et al. (2006); Wapenaar and Snieder (2007); Wapenaar et al. (2010a, b); Snieder and Wapenaar (2010).

Imaging vis-a-vis Inversion Imaging tries to obtain useful (drillable) structural information using large data-redundancy and simple conceptual models, whereas inversion aims at getting values for the physical parameters of the medium, using more involved theory, see ▶ “[Seismic Imaging, Overview](#)”. Buske et al. (2009) give a good introduction to the two approaches, whereas Weglein et al. (2009) discuss some critical underlying questions. Till recently, resolution in seismic imaging suffered from an information-gap as pointed out by Claerbout (1985b): velocity information was being obtained by kinematic analyses for apparent frequencies below ca. 2 Hz and reflectivity was being derived for frequencies above ca. 10 Hz. Recent improvements in tomographic velocity analysis and broadband data acquisition have resulted in increasingly narrowing this gap, which results in improved resolution (Nichols 2012). As shown in the Fig. 12, there is now even an information overlap between the results obtained from these two processing techniques. This, in turn, gives rise to interesting questions regarding the consistency of the high- and low-frequency results that have finally to be combined.

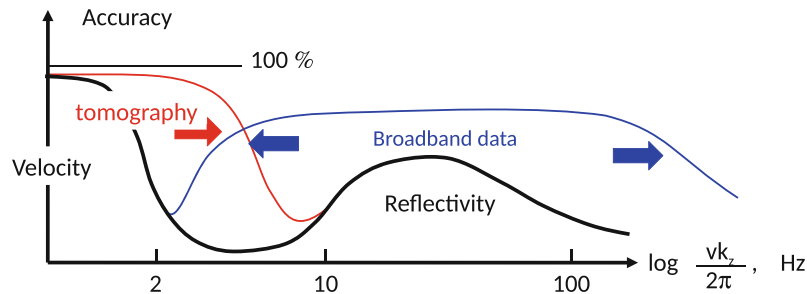
Full wave-form inversion Obtaining the visco-elastic properties of the medium so as to be able to reproduce each seismic/seismological trace *completely* remains the ultimate goal of inversion of seismic/seismological data (see ▶ “[Seismic, Waveform Modeling and Tomography](#)”). This subject is currently the subject of major theoretical and applied research, the latter also profiting from considerable increase in available computational power. In the beginning, efforts were limited to achieving a reasonable match between a selected part (phase) of the observed waveform and the computed synthetic. Given improvements in acquisition, theory, and the computer power, progress is being made to reproduce larger parts of the entire wavetrain – a complete reproduction may though be never achievable. For a quick introduction to this topic, including underlying problems, and related developments in exploration geophysics, see Virieux and Operto (2009); Virieux et al. (2017); Brittan and Jones (2019). Note that *perfect inversion implies perfect imaging – and vice versa!*

Summary

The simple *echo-in-the-well* experiment mentioned at the start needs many physico-mathematical supports to analyze data obtained from the earth’s subsurface. Starting at data acquisition, these acquisition/processing modules yielding the final image resemble a pipeline (flow). Several of these have been explained briefly; for others, cross-references elsewhere in this volume have been provided.

Cross-References

- ▶ [Energy Partitioning of Seismic Waves](#)
- ▶ [Ocean Bottom Seismics](#)
- ▶ [Propagation of Elastic Waves: Fundamentals](#)
- ▶ [Seismic Anisotropy](#)
- ▶ [Seismic Diffraction](#)
- ▶ [Seismic Imaging, Overview](#)
- ▶ [Seismic Instrumentation](#)
- ▶ [Seismic Noise](#)
- ▶ [Seismic Properties of Rocks](#)
- ▶ [Seismic Ray Theory](#)
- ▶ [Seismic Waves, Scattering](#)
- ▶ [Seismic, Ambient Noise Correlation](#)
- ▶ [Seismic, Migration](#)
- ▶ [Seismic, Viscoelastic Attenuation](#)
- ▶ [Seismic, Waveform Modeling and Tomography](#)
- ▶ [Single and Multichannel Seismics](#)
- ▶ [Vertical Seismic Profiling](#)



Seismic Data Acquisition and Processing, Fig. 12 Sketch showing the improvement in resolution in reflection seismics. In black, the famous sketch by Claerbout (1985b), showing the gap between information (accuracy) from velocity analysis and reflectivity. Advances in

tomography (red) and broadband acquisition (blue) have changed the situation essentially to that of an informational overlap. (Figure from Lambare et al. (2014), courtesy EAGE and the author)

References

- Aki K, Richards PG (2002) Quantitative seismology, 2nd edn. University Science Books, CA, USA
- Backus M (1959) Water reverberations – their nature and elimination. *Geophysics* 24(2):233–261
- Beasley C (2008) Simultaneous sources: a technology whose time has come. *Soc Expl Geophys. Expanded abstracts*, 2796–2800
- Bednar J (1996) Coarse is coarse of course unless *The Leading Edge* 15(6):763–764
- Brittan J, Jones I (2019) FWI evolution – from a monolith to a toolkit. *The Leading Edge* 38(3):179–184
- Buske S, Lecomte I, Nemeth T, Operto S, Sallares V (2009) Imaging and inversion – introduction. *Geophysics* 74(6):WCA1–WCA4
- Cherry E (1953) Some experiments on the recognition of speech, with one and with two ears. *J Acoust Soc Am* 25(5):975–979
- Claerbout JF (1968) Synthesis of a layered medium from its acoustic transmission response. *Geophysics* 33(2):264–269
- Claerbout JF (1985a) Fundamentals of geophysical data processing. Blackwell. <http://sepwww.stanford.edu/sep/prof/fgdp5.pdf>
- Claerbout JF (1985b) Imaging the earth's interior. Blackwell. <http://sepwww.stanford.edu/sep/prof/iei2/>
- Curtis A, Gerstoft P, Sato H, Snieder R, Wapenaar K (2006) Seismic interferometry – turning noise into signal. *The Leading Edge* 25(9):1082–1092
- Dean T, Tulett J, Barnwell R (2018) Nodal land seismic acquisition: the next generation. *First Break* 36:47–52
- Dennison AT (1953) The design of electromagnetic geophones. *Geophys Prosp* 1(1):3–28
- Dix C (1955) Seismic velocities from surface measurements. *Geophysics* 20:68–86
- Fink M (1993) Time reversal mirrors. *J Phys D Appl Phys* 26:1333–135. <http://iopscience.iop.org/0022-3727/26/9/001>
- Fink M (1997) Time reversed acoustics. *Phys Today* 50:34–40. <https://doi.org/10.1063/1.881692>
- Garotta R (1983) Simultaneous recording of several vibroseis© seismic lines. *Soc Expl Geophys. Expanded abstracts*, 308–310
- Gülünay N (2003) Seismic trace interpolation in the Fourier transform domain. *Geophysics* 68(1):355–369
- Hegna S, Klüver T, Lima J, Wisloff J (2019) Making the transition from discrete shot records to continuous seismic records and source wavefields, and its potential impact on survey efficiency and environmental footprint. *Geophys Prospect* 67(6):1472–1485
- Helbig K, Thomsen L (2005) 75-plus years of anisotropy in exploration and reservoir seismics: a historical review of concepts and methods. *Geophysics* 70:9ND–23ND
- Hennenfent G, Herrmann F (2008) Simply denoise: Wavefield reconstruction via jittered undersampling. *Geophysics* 73(3):V19–V28
- Herrmann F (2010) Randomized sampling and sparsity: getting more information from fewer samples. *Geophysics* 75(6):WB173–WB187
- Lambare G, Guillaume P, Montel J (2014) Recent advances in ray-based tomography. In: Extended abstracts, 76th annual meeting. EAGE
- Lee M (2008) Comparison of the modified Biot-Gassmann theory and the Kuster-Toksöz theory in predicting elastic velocities of sediments. U.S. Geological survey scientific investigations Report
- Liner C (2004) Elements of 3D seismology. PennWell corporation, OK
- Liu Y, Fomel S (2011) Seismic data interpolation beyond aliasing using regularized nonstationary autoregression. *Geophysics* 76(5):V69–V77
- Menke W (1989) Geophysical data analysis, rev edn. Academic, New York
- Nakayama S, Blacquièrre G, Ishiyama T, Ishikawa S (2019) Blended-acquisition design of irregular geometries towards faster, cheaper, safer and better seismic surveying. *Geophys Prospect* 67(6):1498–1521
- Nichols D (2012) Resolution in seismic inversion. In: Expanded abstracts, 74th annual meeting – workshop. EAGE
- Phinney R, Roy Chowdhury K, Frazer LN (1981) Transformation and analysis of record sections. *J Geophys Res* 86(B1):359–377
- Robinson E (1967) Predictive decomposition of time series with application to seismic exploration. *Geophysics* 32:418–484
- Robinson E (2005) The MIT Geophysical Analysis Group (GAG): 1954 and beyond. *Geophysics*. <https://doi.org/10.1190/1.2000287>
- Robinson E, Treitel S (1964) Principles of digital filtering. *Geophysics* 29:395–404
- Rothman D (1985) Nonlinear inversion, statistical mechanics, and residual statics estimation. *Geophysics* 50(12):2784–2796
- Sheriff RE, Geldart LP (1995) Exploration seismology, 2nd edn. Cambridge University Press, Cambridge, UK
- Snieder R, Wapenaar K (2010) Imaging with ambient noise. *Phys Today* 63(9):44–49
- Treitel S (2005) The MIT Geophysical Analysis Group (GAG): 1954 and beyond. *Geophysics*. <https://doi.org/10.1190/1.1993707>
- Vermeer G (1990) Seismic wavefield sampling. Society of Exploration Geophysicists, Tulsa
- Vermeer GJ (2002) 3-D seismic survey design. Society of Exploration Geophysicists, Tulsa
- Virieux J, Operto S (2009) An overview of full-waveform inversion in exploration geophysics. *Geophysics* 74(6):wcc1–wcc26
- Virieux J, Asnaashari A, Brossier R, Métivier L, Ribodetti A, Zhou W (2017) An overview of full-waveform inversion in exploration geophysics. In: Encyclopedia of exploration geophysics, SEG. pp R1–1–R1–40. <https://doi.org/10.1190/1.9789560803027.entry6>
- Wapenaar K, Snieder R (2007) Chaos tamed. *Nature* 447:643
- Wapenaar K, Draganov D, Snieder R, Campman X, Verdel A (2010a) Tutorial on seismic interferometry, part I. *Geophysics* 75(5):75A195–75A209
- Wapenaar K, Slob E, Snieder R, Curtis A (2010b) Tutorial on seismic interferometry, part II. *Geophysics* 75(5):75A211–75A227

- Weglein A, Zhang H, Ramírez A, Liu F, Lira J (2009) Clarifying the underlying and fundamental meaning of the approximate linear inversion of seismic data. *Geophysics* 74(6):WCD1–WCD13
- Yilmaz O (2001) *Seismic data analysis, processing, inversion and interpretation of seismic data*, 2nd edn. Investigations in geophysics, vol I. Society of Exploration Geophysicists, Tulsa
- Zwartjes P, Sacchi M (2007) Fourier reconstruction of nonuniformly sampled, aliased seismic data. *Geophysics* 72(1):V21–V32